Materials and Design 107 (2016) 341–352

Contents lists available at ScienceDirect

Materials and Design

journal homepage: www.elsevier.com/locate/matdes

Feasibility of mechanical clinching for joining aluminum AA6082-T6 and Carbon Fiber Reinforced Polymer sheets

Francesco Lambiase [a,b,*], Dae-Cheol Ko [c]

[a] Dept. of Industrial and Information Engineering and Economics, University of L'Aquila, via G. Gronchi 18, Zona Industriale di Pile, 67100 (AQ), Italy
[b] University of Naples Federico II, CIRTIBS Research Centre, P.le Tecchio 80, 80125 Naples, Italy
[c] Graduate School of Convergence Science, Pusan National University, Busan 46241, South Korea

ARTICLE INFO

Article history:
Received 4 April 2016
Received in revised form 14 June 2016
Accepted 15 June 2016
Available online 16 June 2016

Keywords:
Mechanical fastening
Joining
Aluminum alloy
Composite
Clinching
CFRP

ABSTRACT

The present paper is aimed at investigating the feasibility of the clinching process for joining aluminum and Carbon Fiber Reinforced Polymer (CFRP) thin sheets. Split dies with sliding sectors were used to make these joints. Different punches were used to assess the effect of the punch-die cavity geometry on the joinability and mechanical behavior of clinched joints. Single lap shear tests were carried out to assess the mechanical behavior of the joints. Morphological analysis was performed to determine the main joint dimensions and the damage produced on the aluminum and the CFRP sheets. The study demonstrates the feasibility of the joining process for these types of materials. In addition, the influence of the punch geometry was clarified. Hybrid clinched joints failed by pullout during the mechanical tests; thus, the undercut was the key parameter influencing this kind of joint. The taper angle should be kept as small as possible since it has a detrimental effect on the undercut dimension and produces greater delamination in the CFRP during the joining process. The increase in the punch diameter involved a higher material flow, leading to joints with larger undercuts, while, on the other hand, it also produced more damage to the CFRP.

1. Introduction

There is a growing use of hybrid metal-composite structures in transportation industries, civil infrastructure and construction. These structures are employed in the automotive and aerospace industries for reducing the product weight, fuel consumption, inertia, and consequently the product performance. For example, in the last few decades, the chassis of many supercars, such as the likes of Ferrari, Lamborghini and McLaren, has combined high-strength steel, aluminum, and carbon-fiber-reinforced plastic. In 2016, the employment of hybrid metal-composite chassis was extended to series production of cheaper vehicles including: Alfa Romeo 4C, BMW 7-series and Chevrolet Corvette Z06, confirming the increasing interest in ultrahigh structures from the automotive industries. Similarly, the employment of composite-metal structures for civil applications is also very promising. Carbon-Fiber Reinforced Polymers (CFRP) can be used to reinforce bridge constructions [1], to increase the flexural rigidity of aluminum beams [2], to repair and strengthen structural components [3–5] and even to protect from fire and thermally insulate lightweight structural materials [6].

From a process point of view, joining such different materials is still a challenging issue because of the great difference between the materials composing such hybrid components. A number of advanced joining techniques have been developed recently to join metals with fiber-reinforced thermoplastics, including friction spot joining [7–9], friction lap welding, [7,10], ultrasonic welding [11], and laser direct joining [12]. These processes produce an adhesion (and in some cases mechanical fastening) between the thermoplastic matrix of the composite and the metal substrate. On the other hand, advanced thermoforming processes, including friction-based stacking [13,14], infrared stacking [15,16], friction riveting [17,18], and flow drilling [19] produce a mechanical interlock between the components and are also suitable for this purpose. Nevertheless, employing the aforementioned processes is mainly restricted to join composites with thermoplastic matrices; on the other hand, they are not suitable for Fiber Reinforced Polymers (FRP) with a thermosetting matrix, since they would involve thermal and mechanical damage of both the fiber and the matrix in the composite.

In this case, mechanical, adhesive bonding and hybrid joining processes, which involve the superposition of a mechanical joint to an adhesively bonded joint, are used [20]. When mechanical joints are employed, different failure types may develop, namely: net tension, cleavage, shear-out, and tear-out (which develop catastrophically), and bearing failure (which develops more gradually). Bearing failure, which results from buckling of the material, is commonly preferred to develop since it ensures a great energy absorbance and higher predictability of the mechanical behavior of the joint. The occurrence of one or another failure type is highly influenced by the geometrical characteristics of the joint

* Corresponding author at: Monteluco di Roio, 67040 (AQ), Italy.
E-mail address: francesco.lambiase@univaq.it (F. Lambiase).

http://dx.doi.org/10.1016/j.matdes.2016.06.061
0264-1275/

such as the "width-to-diameter" and "edge-to-diameter" ratios [21,22]. Large values of these ratios promote bearing failure; small values would result in net-tension and shear-out failure types, respectively [23,24]. The mechanical behavior of mechanical joints can be improved by the employment of z-pins in the composite [25], which can be also used to improve the bearing performances in bolted joints [26]. Mechanical joints ensure high static and dynamic performances and do not require extensive surface preparation. However, these processes usually require preliminary drilling of both the sheets (which often causes damage of the composite material), fiber interruption, and stress concentration. In addition, manual steps such as predrilling and subsequent insertion of extra joining elements represent time-consuming and costly preliminary work, require additional material (the connecting element), and increase the structure weight.

On the other hand, adhesive bonds ensure high stiffness and good fatigue life, since the load is distributed over the entire overlapping area [27–29]; in addition, the composite integrity is not compromised by the presence of holes, leading to lower stress concentration. Nevertheless, adhesive bonding comes with a series of drawbacks, including the non-uniform distribution of stress and strain along the bonding length [30], and the debonding generally initiating at or near one of the bond terminations [31]. The shear strength of adhesive bonds increases with the square of the bonding length [32]. Adhesive bonds are generally characterized by a reduced elongation at break, usually smaller than 10% [33–35] and catastrophic failure. From the process point of view, adhesive bonding requires a long curing time and surface preparation (including etching, grinding, and degreasing) to increase the adhesion between the substrates, resulting in a long processing time, high environmental impact and low standardization of the mechanical behavior. In addition, the bonds' strength highly depends on the adhesive thickness and bonding pressure applied with curing time [36].

Hybrid joining processes represent an interesting alternative to mechanical joining and adhesive bonding processes, since they bring together the advantages of both these categories. Hybrid joining improves both the static [37] and fatigue strength [38], since lower stress concentration develops during service life compared to bolted joints. The mechanical behavior of hybrid joints depends on geometrical characteristics as well as the pitch distance (i.e. distance between bolts in a row) [39]. Because of the large variety of mechanical joining processes, different mechanical connections can be coupled with adhesive bonding, including: bolted [37–39], riveted [40,41], laser riveting, electron-beam formed protrusions [42] and self-pierce rivets [22,43].

So far, a limited number of studies have been performed to assess the suitability of mechanical clinching (MC) for producing metal/Fiber Reinforced Polymers (FRP) joints. This process involves the plastic deformation of the sheets to produce a mechanical interlock by means of a punch and a die. MC has several advantages over common mechanical joining processes, such as simplicity, repeatability, clearness, the absence of external fastening components, and equipment portability. Furthermore, it does not require predrilling of holes or surface preparation, it involves simple and cheap machines, and improves the mechanical behavior of the metal in the joint due to strain hardening. Beyond MC of metal sheets, in recent years a number of investigations has been carried out to evaluate the suitability of MC for joining metals with other materials including thermoplastics [44,45], wood materials [46], FRP with thermoplastic matrix and short fibers [47,48] and thermosetting matrix [49] with long fibers. In this final case, a modified clinching scheme (called hole-clinching) was involved, which required a hole to be pre-drilled in the CFRP sheet before joining by clinching.

This study is aimed at investigating for the first time the suitability of clinching with split dies for joining metal with CFRP sheets with long fibers and thermosetting matrix. During the process, the aluminum sheet is plastically deformed to create an interlock with the CFRP sheet, while any machining operations, for example drilling to make holes in the CFRP composite, were needed for both materials. This allowed the joining time to be drastically reduced (by up to two joints per second). Compared to hole-clinching, the use of split dies would also allow us to overcome coaxiality problems between the hole and the punch, which often affect the mechanical behavior of the connections produced by hole-clinching. Finally, MC could be used in conjunction with adhesive bonding to produce cheaper hybrid joints faster. To study the feasibility of this process for the production of FRP/metal joints, it is essential to analyze how the damage develops in the composite during clinching, the mechanical behavior of the joints, and the influence of the process parameters. To this end, experimental tests were performed on CFRP sheets with a thickness of 1.4 mm and aluminum sheets AA6082-T6 with a thickness of 2.0 mm. The influence of the punch geometry on the geometrical characteristics and damage to the CFRP in the joint neighbors was analyzed. In addition, a series of additional clinching tests was performed by varying the joining force, in order to investigate the material flow and development of damage during the joining process. Mechanical characterization of the joints was performed by conducting single lap shear tests.

2. Materials and methods

2.1. Materials

Rolled sheets of 2.0 mm thick AA6082-T6 were used in this study. This is a precipitation hardenable aluminum alloy with Si and Mg as the main alloying elements. The aluminum sheet was joined with a Carbon Fiber Reinforced Polymer sheet with a thickness of 1.4 mm.

The CFRP laminates were manufactured using plain weave (SK Chemical, UGN200), as shown in Fig. 1. The carbon fiber prepregs (MRC PYROFILTM, TR30S) and a thermosetting epoxy resin (bisphenol-A type epoxy + phenol Novolac type epoxy) were cured for 2 h at 130 °C. The initial thickness of prepreg for a ply was 0.3 mm before the pressure was applied. The final resin content was estimated to be about 53%, as reported in Table 1. The elastic modulus of the CFRP in the 0° direction was 175.3 GPa. Also, the ultimate tensile strength was measured as 962.7 MPa, as reported in Table 2. To compare the mechanical performances of the joints with that of the CFRP sheet, the bearing strength and interlaminar shear strength (ILSS) of the CFRP material were determined according to ASTM D5961-04 [50] and ASTM D3846 [51], respectively.

2.2. Clinching equipment

Clinched joints were performed by means of a portable clinching machine model Python by Jurado srl (Rivotorto (Perugia), Italy). Different punches were used by varying the taper angle and the pin diameter. The tool pin had a fillet radius of 0.2 mm to reduce the stress on the aluminum alloy, which is characterized by a low ductility [52,53]. Table 3 summarizes the geometries of the adopted tools. A split die comprising three sliding sectors was used in the investigation. Preliminary tests were performed on similar dies having a smaller die anvil depth (h); however, these joints were characterized by reduced mechanical behavior rather than greater formation of crumbles within the die. Thus, the investigation was performed on dies of $h = 1.1$ mm.

The geometrical characteristics of the dies are reported in Fig. 2. The joints were performed using the maximum available joining force ($F_j = 28.8$ kN) of the adopted machine, placing the aluminum at the punch side and the CFRP sheet at the die side.

2.3. Mechanical characterization of the joints

Single lap shear tests were conducted on a Universal Test machine model 322.31 by MTS with a load capacity of 250 kN using 25 kN full-scale under quasi-static conditions (constant speed 1 mm/min) at room temperature. The geometry and specimen dimensions are reported in Fig. 3a. Five replicates were performed for each joining condition

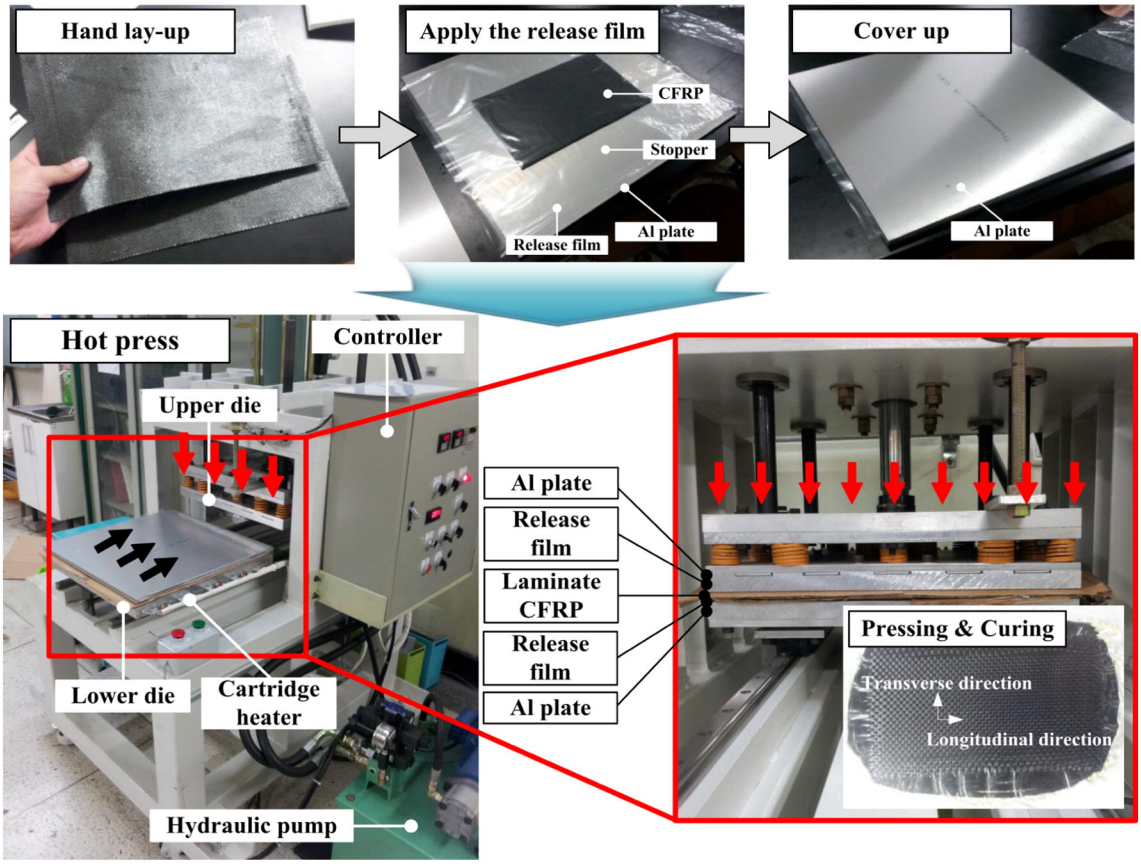

Fig. 1. Manufacturing process of CFRP laminates.

and the average and standard deviation of the shear strength F_r (maximum load recorded during the shear test) and absorbed energy W were determined, as schematically depicted in Fig. 4.

To examine the deformation of the joint during the single lap shear tests, a new type of specimen was designed, as schematized in Fig. 3b. The specimen is constituted by two-half joints (which were sectioned after joining by clinching). This shape constrained the rotation of the specimen around the joint during the shear test. The shear test was thus recorded using a 16-bit DSLR camera model D5200 by Nikon with a resolution of 6000 × 4000.

2.4. Morphological characterization of the joints

The cross-section of the joints performed under different processing conditions (e.g. pin geometry or joining force) was analyzed using an optical microscope (DM IR microscope, Leica) under reflective light. The joints were previously cut in the middle by means of a low-speed saw with diamond blade. For each punch the main geometrical parameters, namely the undercut t_s and the neck thickness t_n depicted in Fig. 5, were measured.

3. Results and discussion

Fig. 6 shows the presence of CFRP crumbles among the die sectors and die anvil interstices. Actually, during clinch joining, the die-sided material is highly compressed; thus, when a relatively brittle material (such as the CFRP) is placed at the die-side, some crumbles may separate from the rest of the sheet and remain entrapped in the die. According to experimental observations, when the punch with the smaller pin diameter (d = 3 mm) was used, no crumbles were shown after joining; on the other hand, increasing the pin diameter involved a greater separation of crumbles entrapped within the die interstices. Indeed, larger punches involved a greater material flow; thus, the CFRP material was forced to flow within the die interstices and remained entrapped.

3.1. Material flow

To understand the material flow and the development of damage on the CFRP sheet, a series of clinching tests were performed, varying the joining force F_j in the range 7.2–28.8 kN. Fig. 7 shows the cross-sections of the clinched joints with varying F_j. As can be inferred, the CFRP sheet under the aluminum bulge delaminates during the early phase of clinch joining (offsetting), as shown in Fig. 7a–b. During this phase, the CFRP is mainly subjected to bending load. For larger punch strokes (Fig. 7c), the CFRP under the aluminum sheet is upset against the underlying die anvil and fractures definitely. Thus, a hole in the CFRP sheet is formed since there is a complete cut of the carbon fibers surrounding the aluminum bulge (Fig. 7d). The aluminum bulge is also upset between the

Table 1
Manufacturing conditions of CFRP.

Type of woven fabric	Thickness of laminate [mm]	Number of plies	Fiber volume fraction [%]	Lay-up angle [deg]
Plain weave (3 K)	1.4	7	53.3 ± 0.45	0

Table 2
Mechanical properties of CFRP and AA6082-T6 alloy.

Material	Elastic modulus [GPa]	Ultimate tensile strength [MPa]	Flow stress [MPa]	Bearing strength [MPa]	ILSS [MPa]
AA6082-T6	69	340	$\sigma_p = 467\varepsilon^{0.098}$	–	–
CFRP	175.3	962.7	–	366	19.1

Table 3
Geometrical parameters of adopted punches.

Punch	Pin Diameter, d [mm]	Taper Angle, α [deg]
P4–12	4	12
P3–6	3	6
P4–6	4	6
P4.5–6	4.5	6

punch and the CFRP and begins to spread radially, compacting the walls of the CFRP hole (Fig. 7e and f). During the upsetting phase, the increase in the joining force F_j results in an increase of the material flow (growth of undercut) and high radial displacement of the sliding sectors. Thus, the aluminum spreads radially and compacts the delaminated area, resulting in a partial damage recovery. As a result, the side walls of the CFRP hole are highly compressed.

3.2. Geometrical characterization of the joints

The mechanical behavior of clinched joints depends on geometrical factors such as the joint diameter, the length of contact arc [45], the neck thickness and undercut dimensions [54], the damage which may develop during the joint formation [53], and the local flow stress (owing to the strain hardening). All these characteristics are determined by the geometry of the clinching tools as well as the process temperature which improves the material formability [52].

When clinching is used to join aluminum sheets, punches with a taper angle are preferable to enable easy extraction of the punch from the aluminum sheet after joining. Tapered pins also allow a reduction of the damage in materials with low ductility, e.g. aluminum alloys or high-strength steels [52,55], since they allow the shear stress developing on the punch-sided sheets to be relieved. However, when clinching is used to join metal sheets with fiber-reinforced polymers, it is preferable to develop a high shear stress in the composite sheet in order to prevent excessive damage and delamination. Thus, the choice of the pin taper angle should be a trade-off among these different requirements.

The employment of larger tapered angles α results in higher compressive stress during the offsetting phase, which reduces the material flow and thus influences the joint geometry. This is evident when comparing the geometries of joints P4–6 and P4–12, as shown in Fig. 8a. Here, the increase in the taper angle results in a reduction in the undercut t_s from 0.14 mm to 0.08 mm, while it comes with an increase in the neck thickness t_n from 0.78 mm to 0.88 mm.

Comparing the joints performed with punches P3–6, P4–6, and P4.5–6, it is evident that increasing the pin diameter results in an increase of the undercut t_s, as depicted in Fig. 8b. Indeed, larger pins involve higher material flow during clinch joining, which finally results in larger undercuts. On the other hand, negligible variations were found in the neck thicknesses of joints produced when varying the pin diameter.

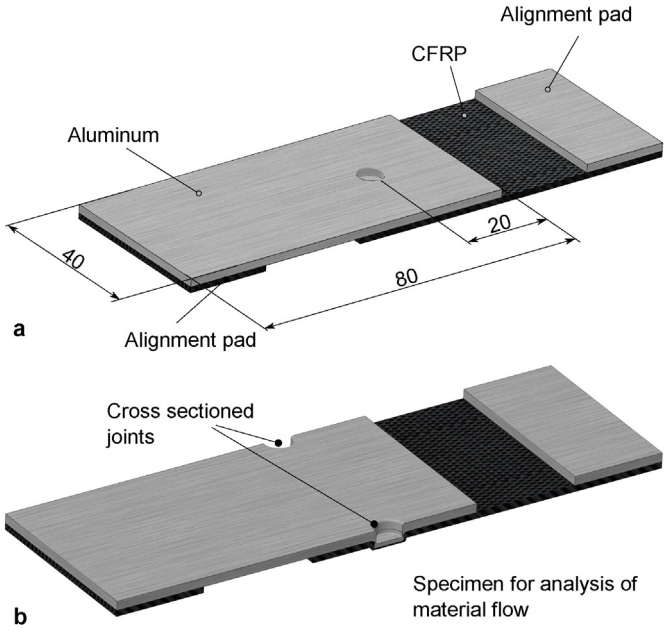

Fig. 3. Schematic of the specimens used for characterization tests: (a) single lap shear test and (b) "two halves" specimen used for analysis of material flow of cross-section.

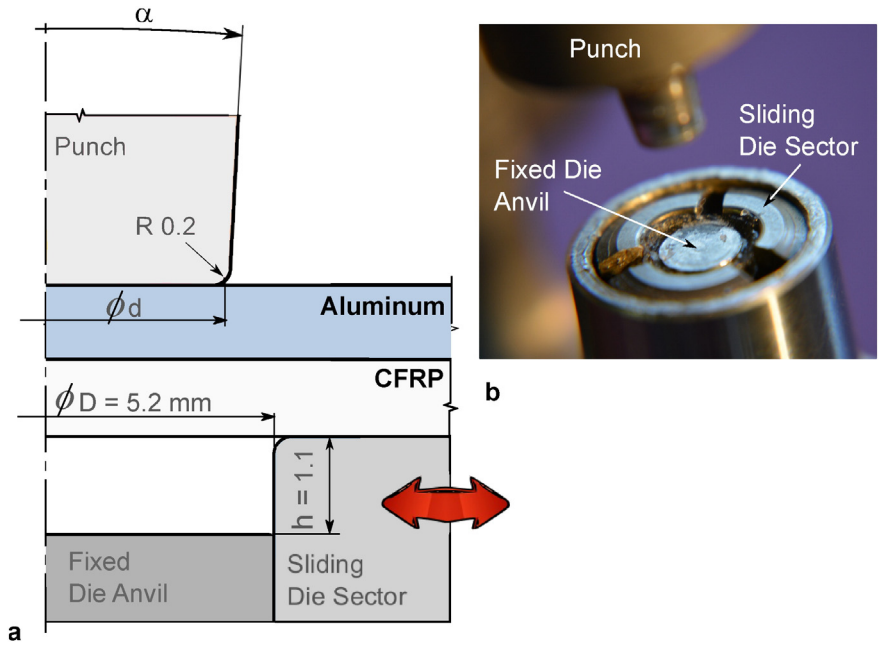

Fig. 2. (a) Schematic of the adopted clinching tools; (b) macrograph of the clinching tools.

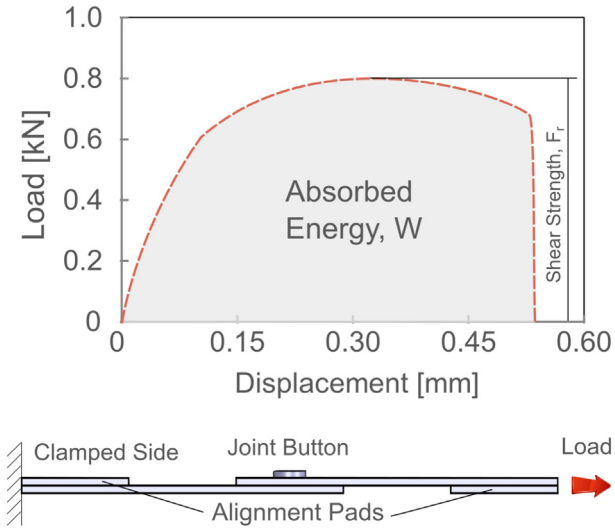

Fig. 4. Mechanical characteristics of clinched joints recorded during single lap shear tests.

3.3. Morphological analysis

During the clinch joining operation, the sheets are subjected to high deformations (more than 100% [56]). Such conditions may dramatically compromise the integrity of the sheets in the key-hole, especially when low ductility materials such as the AA6082-T6 alloy sheets involved are used and even when brittle materials such as CFRP sheets are involved. Thus, the proper selection of the clinching tools is needed to prevent the onset and development of cracks, rather than maximizing the characteristic dimensions of the clinched joints. As can be observed in Fig. 9, the aluminum was never damaged regardless of the type of tool. On the other hand, while clinching metal with Fiber Reinforced Polymers by conventional clinching tools, the CFRP hole was produced to allow the metal flow and consequent fastening development. Nevertheless, the hole formation should be controlled in order to avoid excessive delamination in the composite sheet.

Fig. 9 compares the cross-section of clinched joints produced with different punches. As can be inferred, increasing the pin diameter leads to greater damage of the CFRP in the bulge neighbors. This is due to a higher hydrostatic stress developing during the offsetting phase, which delays the cut of the fibers, leading to a higher composite delamination.

Comparing Fig. 9b with Fig. 9d, it is evident that the increase in the taper angle α involves greater damage on the CFRP sheet, which is due to the delay in the fibers cut along the developing hole owing to higher hydrostatic stress produced during the offsetting phase.

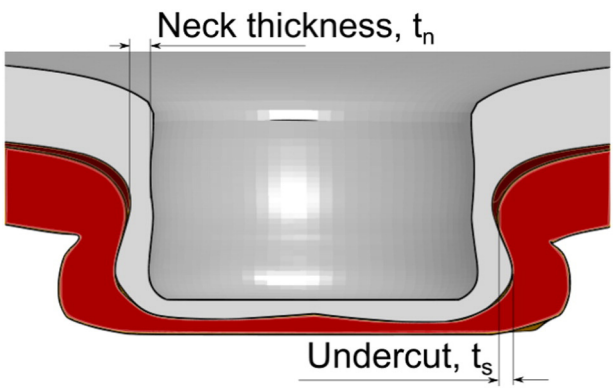

Fig. 5. Main geometrical characteristics of clinched joints.

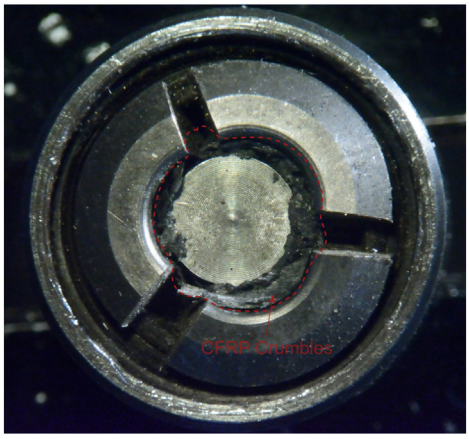

Fig. 6. Crumbles entrapped in the die.

The effect of the punch geometry on the damaged area is also depicted in Fig. 10, which shows the die-sided view of the CFRP sheet after clinching. As can be inferred, the punch P3–6 allows the damaged area to be restricted, while in the other cases, much greater damage of the CFRP is shown.

3.4. Single lap shear tests

During the single lap shear tests, all the examined joints failed by pull-out followed by bearing of CFRP regardless of the type of punch used. This kind of failure consists in the ejection of the aluminum bulge from the composite housing owing to small values of undercut as compared to neck thickness, as schematically depicted in Fig. 11. During the single lap shear tests, the clinched joint is subjected to a rotation given by distance r between the shear load acting on the aluminum sheet (F_s) and the resulting contact force exerted by the CFRP hole (P_x). Such a rotation is balanced by the contact force exerted by the undercut on the opposite side of the key-hole (P_y). When the peak of load is reached, evident deformation of the aluminum bulge can be observed, leading to the ejection of the aluminum bulge from the CFRP sheet. According to Fig. 12, which depicts the deformation of a double-halves specimen during the shear tests, after the onset of the peak, the joints hold a high mechanical resistance, which gradually reduces with large deformation of the aluminum bulge.

Load-displacement curves of clinched joints performed with different punches are reported in Fig. 13a. All the joints failed after a high elongation before rupture, resulting in high-absorbed energy. This was due to the large sliding of the aluminum bulge over the CFRP hole.

The increase in the taper angle α has detrimental effects on both the shear strength F_r and the absorbed energy W (Fig. 13b and d). Indeed, increasing the taper angle results in both the reduction of the undercut dimension (as reported in Fig. 8) and increase of the CFRP damage (as shown in Fig. 9).

The influence of the pin diameter d on the mechanical behavior of clinched joints does not show a monotonic trend (Fig. 13c and e). Indeed, both the shear strength and the absorbed energy slightly decrease while increasing d from d = 3 mm to d = 4 mm (P4–6) and then increase greatly for d = 4.5 mm (P4.5–6). The mechanical behavior of clinched joints failing by pullout is highly influenced by the undercut dimensions, which increases with the pin diameter. However, the load-bearing capacity of the CFRP hole also depends on the damage condition of the material surrounding the aluminum bulge. As discussed in the analysis of morphology section, the damage increases with the pin diameter. Therefore, the trend of the shear strength and absorbed energy suggests that the effect of the increase in CFRP damage is predominant until the pin diameter is smaller than d = 4 mm. On the other hand, for larger values of pin diameter, i.e. d = 4.5 mm, the increase in the

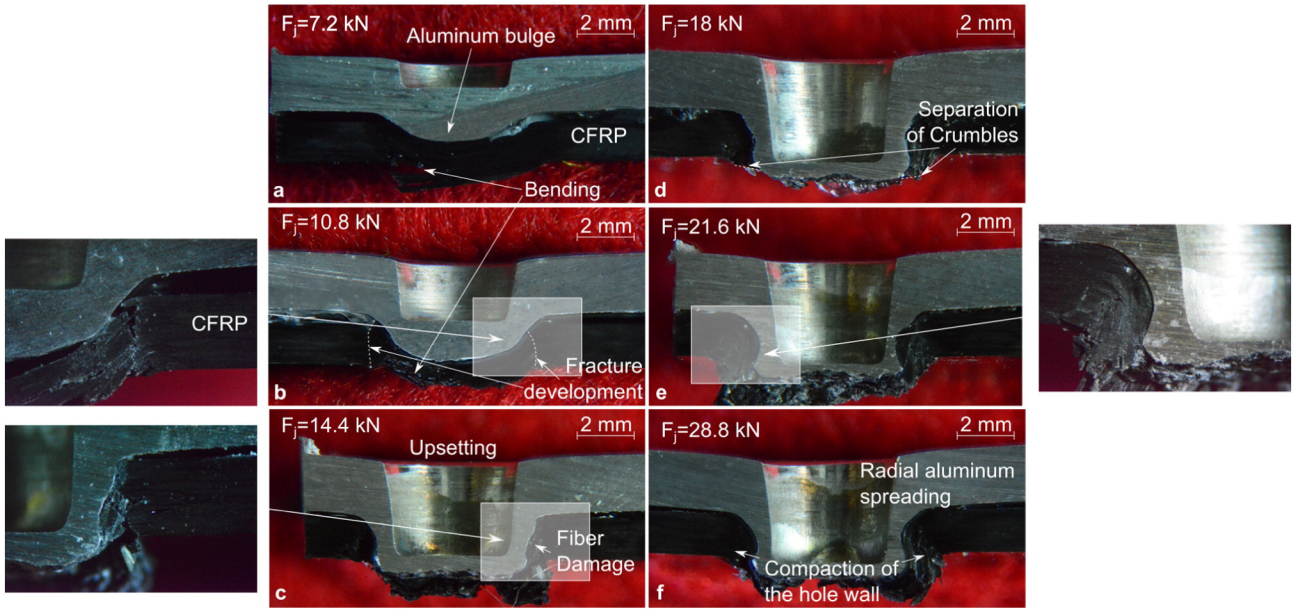

Fig. 7. Cross-section of clinched joints performed with punch P4–6 at different joining forces F_j: (a) $F_j = 7.2$ kN, (b) $F_j = 10.8$ kN, (c) $F_j = 14.4$ kN, (d) $F_j = 18$ kN, (e) $F_j = 21.6$ kN and (f) $F_j = 28.8$ kN.

undercut becomes predominant, leading to a drastic increase in the mechanical behavior of the joints.

In the joints produced with punches with $\alpha = 6°$, the CFRP hole showed a sharp and regular cut of the carbon fibers with reduced delamination in the joint neighbor, as shown in Fig. 14. These joints showed a large bearing region in the direction of shear load, which confirms their high mechanical behavior.

3.5. Mechanical performances of joints

In order to compare the mechanical behavior of hybrid Al/CFRP clinched joints with those produced by other joining processes, the "nominal shear strength", "bearing stress" and "joint efficiency" (expressed as the ratio of the joint failure load to the failure load of the lower strength base material) were calculated.

The nominal shear strength of the joints was calculated as the ratio of the shear strength of the joints F_r to the reference joint overlapping area A_o. As suggested by clinching machines manufactures, A_o is given by the minimum spacing between two joints. This area can be calculated by geometrical considerations: Fig. 15.

Based on these considerations, the reference areas for the evaluation of the "nominal shear strength of joints": A_o, "bearing stress": A_b and "joint efficiency": A_x (expressed as the ratio of the joint failure load to the failure load of the lower strength base material) were calculated, as reported schematically in Fig. 16.

3.5.1. Bearing strength

To evaluate the effectiveness of clinching for joining AA6082-T6/CFRP hybrid joints, and compare the joints strength with the tensile strength of the CFRP composite, the maximum bearing stress $\sigma_b = F_r/A_b$ of the clinched joint was calculated. For clinched connections, a sound value of A_b can be calculated by Eq. (1) [45]:

$$A_b = h \cdot (d + 2t_n + t_s) \quad (1)$$

where: h is the Al/CFRP penetration depth, d, t_n and t_s are the punch diameter, the joint neck thickness and undercut, respectively. Using Eq. (1), the bearing stress of the joints made by different tools was calculated and reported in Fig. 17a. The bearing stress slightly decreases with the increase of the punch diameter, while it is more affected by the taper angle of the tool due to the low shear strength of the joints made by the "P4–12" tool. The values of bearing stress of the clinched joints are lower that of the CFRP composite (366 MPa, as reported in Table 2); thus, the failure of the joints starts from the connecting

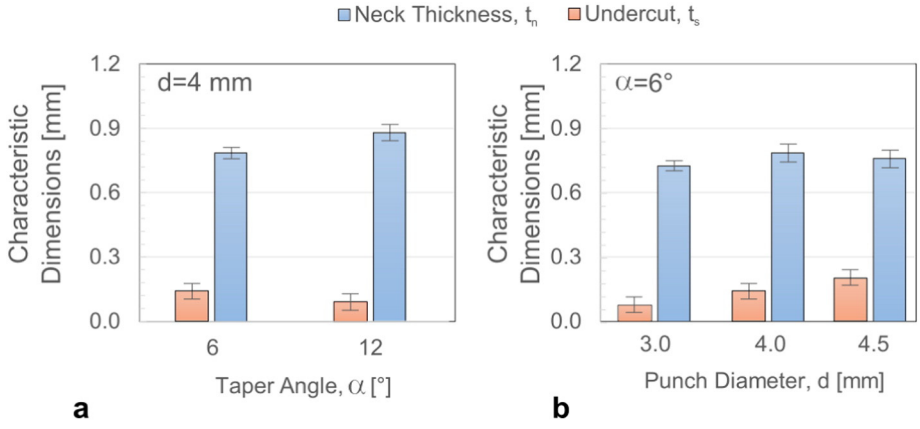

Fig. 8. Influence of the (a) taper angle and (b) punch diameter on the characteristic dimensions of clinched joints.

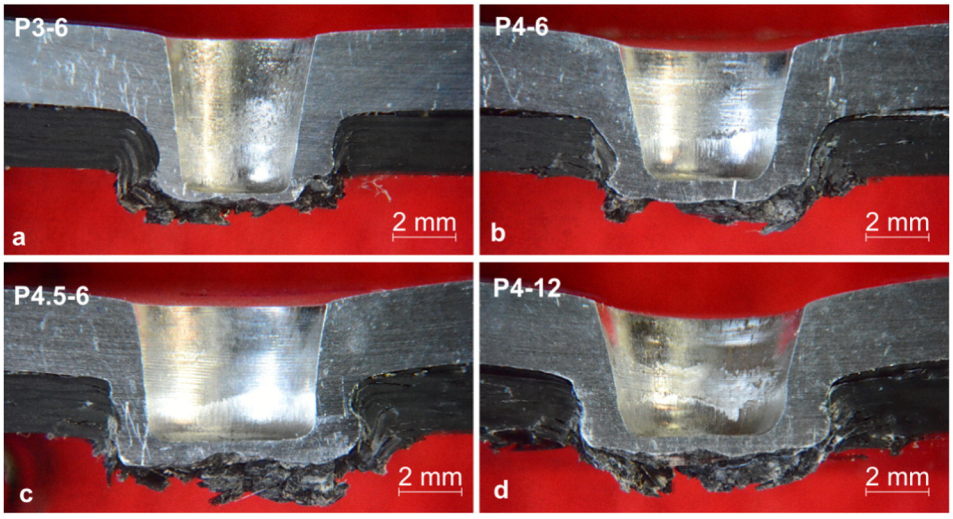

Fig. 9. Cross-section of the joints performed with different tools: (a) P3–6, (b) P4–6, (c) P4.5–6, and (d) P4–12.

element (aluminum bulge) rather than in the CFRP. Nevertheless, at the end of the shear tests, the Al/CFRP penetration depth h reduces (since the aluminum bulge is pulled out from the CFRP hole); thus, the bearing stress increases leading to a partial bearing of the CFRP composite.

The ratio of the bearing stress of the joints to the bearing strength of the CFRP composite σ_b/σ_{CFRP} can be used as an index of the effectiveness of the joining process. Here, the highest values of $\sigma_b/\sigma_{CFRP} = 66\%$ were reached by the joints made with the "P3–6" punch. In this type of joints, other than the selection of the clinching tools, this index is highly influenced by the thickness and mechanical characteristics of the metal component (since the connection element is part of the metal sheet) other than the bearing strength of the die-sided material ($\sigma_b/\sigma_{PC} = 100\%$ was found in [45] when joining AA6082-T6 with polycarbonate sheets). Thus, higher values of σ_b/σ_{PC} ratio can be expected when joining higher strength metals including AA7075 alloys, steels and high strength steels with CFRP composites.

3.5.2. Nominal shear strength

In order to compare the mechanical performances of the clinched joints with adhesive bonds, normalized values of the strength were calculated. The nominal shear strength σ_s was calculated was calculated as: $\sigma_s = F_r/A_o$, where $A_o = (a + b)^2/4$.

As can be observed in Fig. 17b, clinched joints with the smaller taper angle ($\alpha = 6°$) were characterized by similar values of σ_s that ranged within 11.7 and 12.9 MPa, while the joints performed with the larger taper angle ($\alpha = 12°$) were characterized by almost half of the nominal

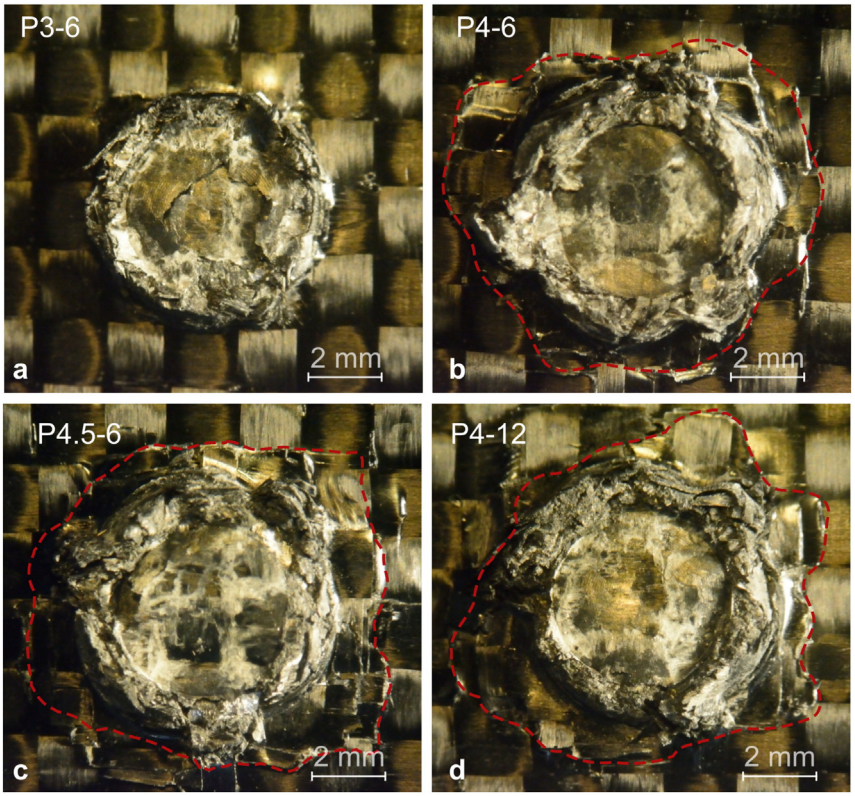

Fig. 10. Die-sided view of clinched connections performed varying the clinching tools: (a) P3–6, (b) P4–6, (c) P4.5–6, and (d) P4–12.

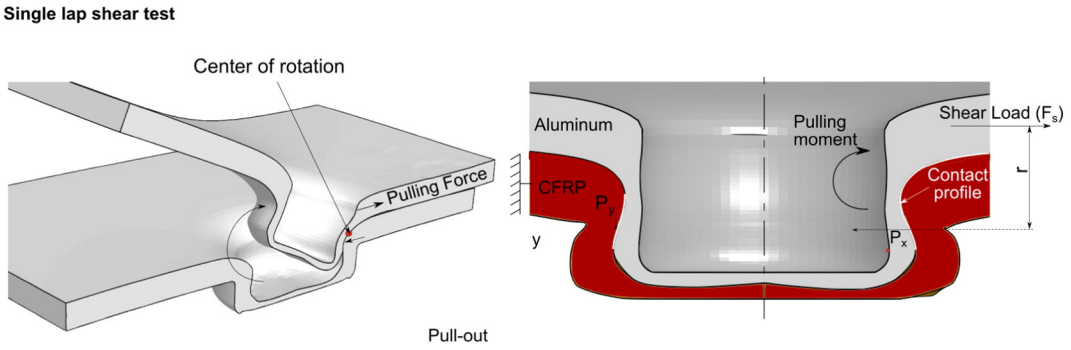

Fig. 11. Main loads acting on clinched joints during single lap shear test.

shear strength: $\sigma_s = 5.8$ MPa. Indeed, the joints made by the "P4–12" punch showed a much lower value of F_r and, at the same time, a large bulge diameter b, which resulted in larger values of A_o.

The mechanical behavior of the joints was compared to those of adhesive bonding process. Common adhesives used in automotive and aircraft manufacturing are characterized by a maximum shear strength ranging between 12 MPa of J-135 [34] and 31.9 MPa of FM73 [37]. Thus, compared to adhesive bonding processes, the clinched joints apparently showed lower values of nominal shear strength. However, these are only reference values since the mean strength at failure of adhesive bonds depends on temperature, humidity, adherent materials, specimen thicknesses, and especially the overlapping length [37]. Indeed, the stress follows a "U-shape" distribution in the bond length direction. Thus, the average stress at failure of the bond is much lower than the maximum shear strength of the adhesive itself. Therefore, for a clearer comparison, comparative experimental tests involving adhesive bonds would be more explanatory.

3.5.3. Joint efficiency

To compare the mechanical behavior joints made by different processes, the joint efficiency J, was also calculated. This parameter is defined as the ratio of the joint failure load to the failure load of the lower strength base material; thus, J represents a design parameter to determine the number of joints in structural applications. In this case, the aluminum was used as the reference material since it has a lower fracture strength 340 MPa vs. 962.7 MPa of CFRP. To this end, the cross sectional area of the aluminum A_x (reported in Fig. 16c) was used to evaluate the failure load of the aluminum coupons.

The Joint efficiency of clinched joint for CFRP was evaluated as 11.6–25.5%, as shown in Fig. 17c. Joint efficiency was not increased as a proportion of the joined area. It means that the geometrical interlocking shape, i.e. neck thickness and undercut in clinched joint, is important to increase the joint strength and joint efficiency.

The joint efficiency of bolted connections is proportional to the bearing and shear strength of the laminate, the width-to-diameter ratio but

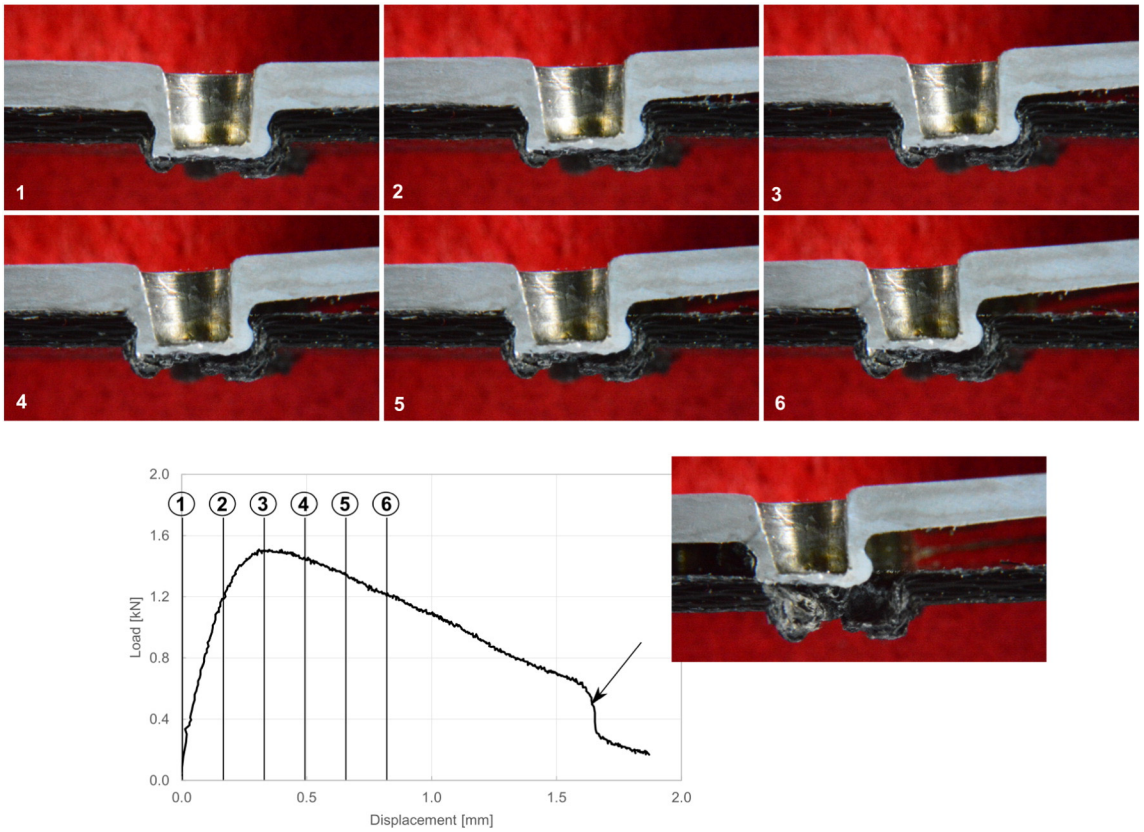

Fig. 12. Deformation of the clinch joint: configuration of double-half joint (punch P3–6).

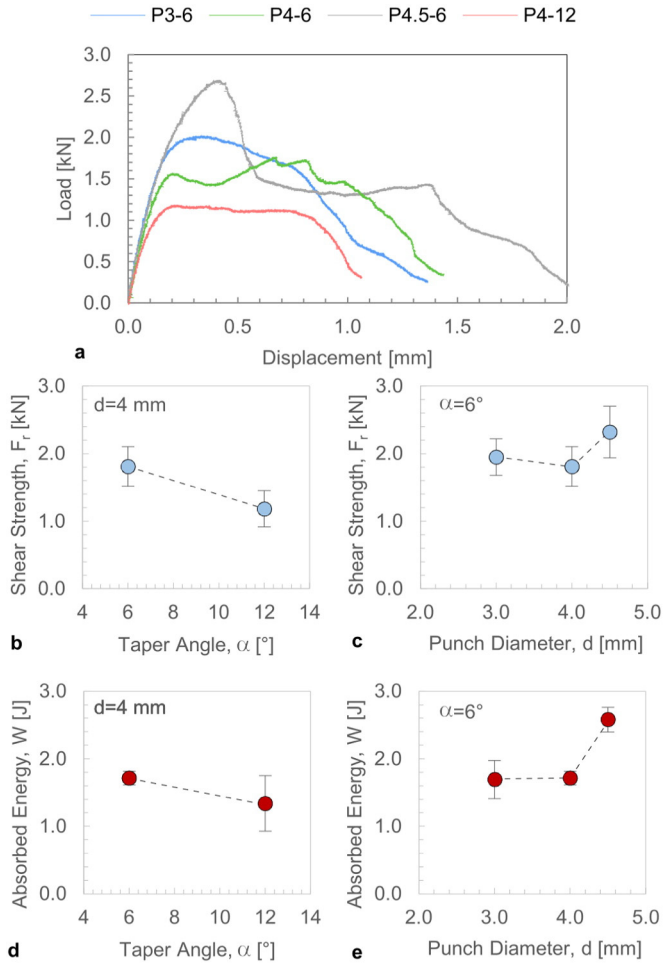

Fig. 13. Influence of the punch geometry on mechanical behavior of clinched joints varying the punch geometry: (a) comparison of load-displacement curves, (b) influence of taper angle on shear strength, (c) influence of punch diameter on shear strength, (d) influence of taper angle on absorbed energy, and (e) influence of punch diameter on absorbed energy.

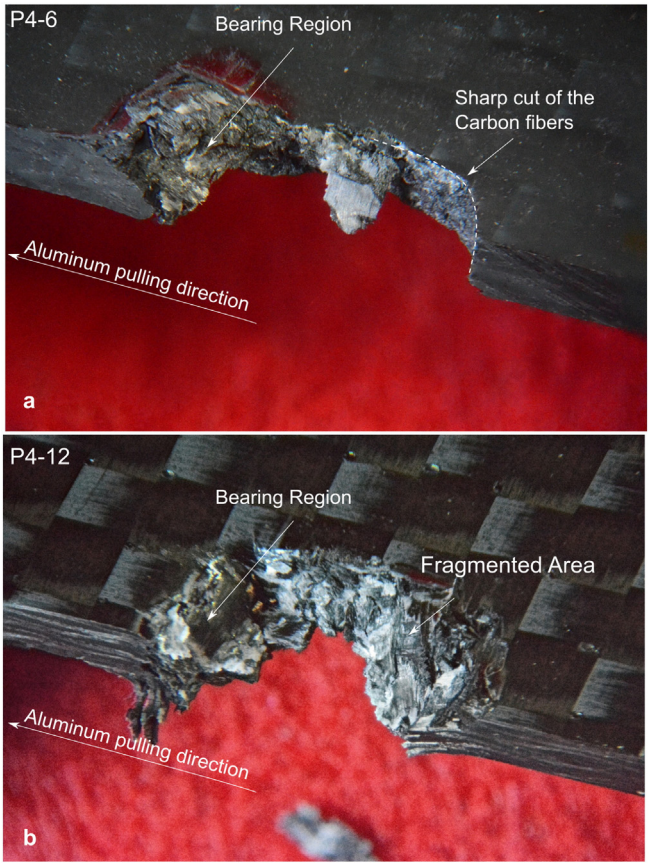

Fig. 14. Influence of taper angle on CFRP damage after single lap shear test: (a) smaller taper angle α = 6° and (b) larger taper angle α = 12°.

also on the notched strength of the laminate [57]. The joint efficiency of bolted connections made on CFRP/metals hybrid joints typically ranges between 45% - 100% [58,59].

The joint efficiency of adhesive bonds is highly affected by several parameters including the adhesive and adherend materials, the overlap length, and the adhesive and adherend thickness. Considering the results reported in [60] the joint efficiency of adhesive bonded joints ranges between 20% and 30% for bonds having a length of 50 mm. However, even smaller values are obtained by adhesive bonds having smaller overlapping length.

Therefore, the lap shear strength of clinched joint was evaluated in about 50% of bolted joints, while clinched joints showed similar joint efficiency of adhesive bonds. Thus, the joint strength of all experiment, except P4–12 case, showed the potential as a joining method for CFRP and metal structures, while even higher performances can be expected by using higher strength material for the metal partner or larger clinching dies.

3.5.4. Comparison with other fast joining processes

The growing need of joining different materials is pushing the research to develop fast joining processes that require lower pretreatments, such as Self-Pierce Riveting SPR and hole clinching.

Compared to SPR, the joint diameters being equal, clinching produces weaker joints. This was confirmed by comparing the experimental results to the shear strength of the self-pierce riveted CFRP/Al joints reported in [22,61], which ranged between 3.5 and 4.0 kN. However, the adoption of SPR involves a significant increase in weight (especially for lightweight structures), higher forming forces (that are almost three times those required by clinching), and an increase of the joining process cost (due to the relatively high cost of self-pierce rivets). On the other hand, if this comparison is performed using the same joining force (using larger joints or multiple-joints per stroke), clinching allows one to achieve equal or even higher values of shear strength compared to SPR. In addition, the mechanical behavior of clinched connection is more heavily influenced by the yield strength and thickness of the metal sheet, since it also represents the connecting element. This suggests that even better results can be obtained when joining thicker

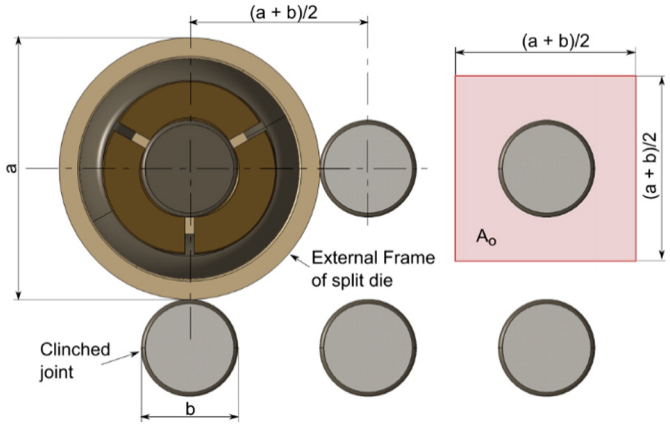

Fig. 15. Geometrical calculation of the reference joint area.

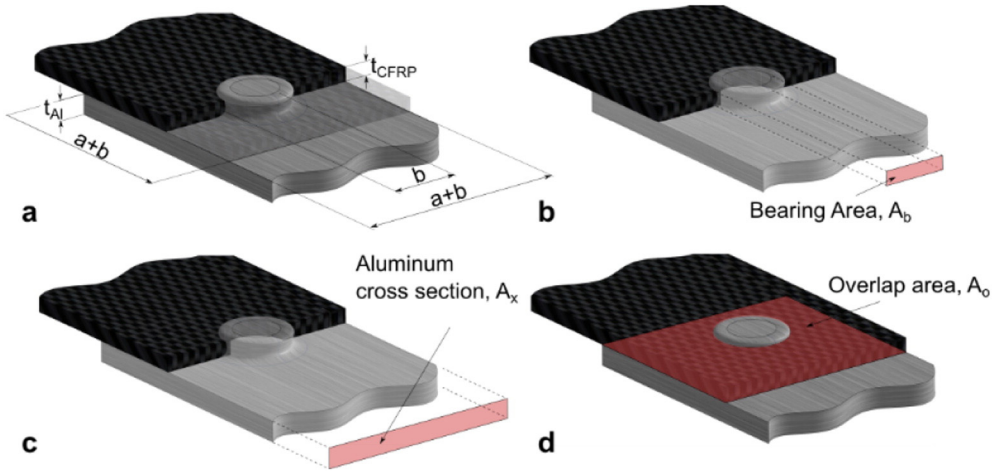

Fig. 16. (a) Main specimen dimensions; reference areas for calculation of (a) bearing stress; (c) joint efficiency and (d) nominal shear strength of joints.

sheets or higher strength materials (e.g. aluminum series 7xxx, steels and high strength steels) to the CFRP sheets.

The clinched joints achieved here (especially those produced using punches "P4.5–6" and "P4–12") showed certain damage in the CFRP, as shown in Fig. 9. Thus, further experiments were performed by drilling a hole in the CFRP, followed by clinching with a split die. This method, also called hole-clinching [49], was expected to reduce the delamination in the CFRP material. To this end, holes with different hole diameters $d_h = 5$ mm, $d_h = 5.5$ mm and $d_h = 6$ mm were made in the CFRP.

Fig. 18 shows the cross-section of a joint produced by hole clinching (with $d_h = 5.5$ mm). Similar conditions were found in the joints made on CFRP with holes of different diameters. Although lower delamination of the CFRP sheet was observed, hole-clinching produced a deep fracture in the aluminum bulge that compromised the mechanical performance of the joint. The occurrence of fracture was due to the low ductility of the aluminum alloy [55] other than the reduced aluminum thickness. When hole-clinching was used, the aluminum was not supported by the CFRP during the offsetting phase. This led to the development of high tensile stress in the aluminum bulge side-walls, in agreement with experimental findings reported in [53]. The presence of the hole in the CFRP prolonged the offsetting phase (by the thickness of the CFRP), with the consequent development of fracture in the aluminum sheet.

4. Conclusions

The present investigation was aimed at verifying the suitability of mechanical clinching for producing hybrid CFRP–aluminum joints using extensible dies. Different geometries of the clinching tools were tested by varying the pin diameter and the taper angle. Geometrical and morphological analysis revealed the influence of the punch geometry and damage on the clinched joints. Single lap shear tests were carried out to assess the mechanical behavior of the joints. In addition, a new type of specimen consisting of a doubled half joint was developed to enable the observation of the clinched joint behavior during the shear test. The main findings of the research are as follows:

- split dies are suitable to join thin aluminum and CFRP sheets;
- all the joints failed by pullout mode; thus, the key parameter determining the mechanical behavior of the joints was the undercut, rather than the delamination of the CFRP near the key-hole;
- punches having large taper angles resulted in smaller undercuts and greater damage in the CFRP, which had a marked effect on the mechanical behavior of the joints. Reducing the punch taper angle from 12° to 6° allowed an increase in the shear strength of 50%.
- the increase in the pin diameter (d) resulted in increase in the undercut (since the greater material flow) but also greater delamination on the CFRP. This was reflected on the mechanical behavior of the joints. Indeed, for the intermediate value of the punch diameter, the joint strength and absorbed energy showed a minimum, wile for the largest punch (d = 4.5 mm) the best mechanical performances were achieved.
- the nominal shear strength of the joints, calculated as the ratio of the shear strength to the reference joint area ranged from 5.8 MPa to 12.9 MPa.
- the bearing stress of the joints ranged from 26% (96 MPa) to 66% (244 MPa) of that of the CFRP composite (366 MPa).

Acknowledgements

The authors would like to thank Jurado (Rivotorto di Assisi, Italy) for providing the extensible dies used in this research. The authors would also like to thank Mr. Giuseppe Organtini (DIIIE - University of L'Aquila)

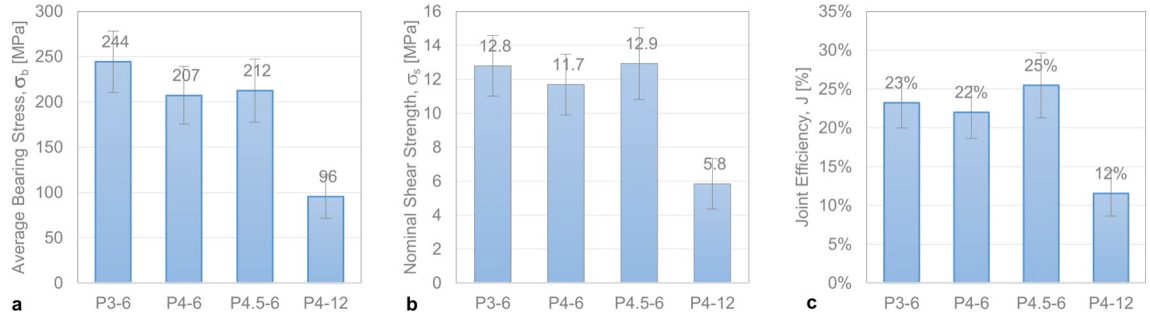

Fig. 17. (a) Bearing strength; (b) nominal shear strength and (c) joint efficiency of clinched joints made by different tools.

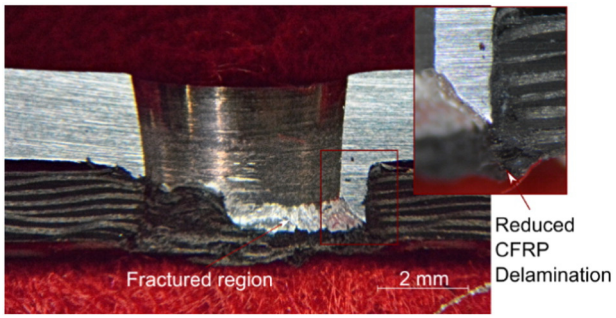

Fig. 18. Cross section of a joint produced by hole-clinching.

for the contribution during the setup and conduction of the experimental tests. This work was also supported by the National Research Foundation of Korea (NRF) Grant funded by the Korean government (MSIP) (No. 2012R1A5A1048294). Finally, the authors are grateful to prof. Antonio Langella from University of Naples "Federico II" for his help during mechanical characterization of composite materials.

References

[1] Y. Zhou, H. Fan, K. Jiang, M. Gou, N. Li, P. Zhu, et al., Experimental flexural behaviors of CFRP strengthened aluminum beams, Commun. Strateg. 116 (2014) 761–771.
[2] F. Meng, W. Li, H. Fan, Y. Zhou, A nonlinear theory for CFRP strengthened aluminum beam, Commun. Strateg. 131 (2015) 574–577.
[3] X.-L. Zhao, L. Zhang, State-of-the-art review on FRP strengthened steel structures, Eng. Struct. 29 (2007) 1808–1823.
[4] J.G. Teng, T. Yu, D. Fernando, Strengthening of steel structures with fiber-reinforced polymer composites, J. Constr. Steel Res. 78 (2012) 131–143.
[5] K.A. Harries, A.J. Peck, E.J. Abraham, Enhancing stability of structural steel sections using FRP, Thin-Walled Struct. 47 (2009) 1092–1101.
[6] S. Christke, A.G. Gibson, K. Grigoriou, A.P. Mouritz, Multi-layer polymer metal laminates for the fire protection of lightweight structures, Mater. Des. 97 (2016) 349–356.
[7] J.V. Esteves, S.M. Goushegir, J.F. dos Santos, L.B. Canto, E. Hage, S.T. Amancio-Filho, Friction spot joining of aluminum AA6181-T4 and carbon fiber-reinforced poly(phenylene sulfide): effects of process parameters on the microstructure and mechanical strength, Mater. Des. 66 (2015) 437–445.
[8] S.M. Goushegir, J.F. dos Santos, S.T. Amancio-Filho, Friction spot joining of aluminum AA2024/carbon-fiber reinforced poly(phenylene sulfide) composite single lap joints: microstructure and mechanical performance, Mater. Des. 54 (2014) 196–206.
[9] S.T. Amancio-Filho, C. Bueno, J.F. dos Santos, N. Huber, E. Hage, On the feasibility of friction spot joining in magnesium/fiber-reinforced polymer composite hybrid structures, Mater. Sci. Eng. A 528 (2011) 3841–3848.
[10] F.C. Liu, J. Liao, K. Nakata, Joining of metal to plastic using friction lap welding, Mater. Des. 54 (2014) 236–244.
[11] F. Balle, S. Huxhold, G. Wagner, D. Eifler, Damage monitoring of ultrasonically welded aluminum/CFRP-joints by electrical resistance measurements, Protein Eng. 10 (2011) 433–438.
[12] K.W. Jung, Y. Kawahito, M. Takahashi, S. Katayama, Laser direct joining of carbon fiber reinforced plastic to zinc-coated steel, Mater. Des. 47 (2013) 179–188.
[13] A.B. Abibe, M. Sônego, J.F. dos Santos, L.B. Canto, S.T. Amancio-Filho, On the feasibility of a friction-based staking joining method for polymer–metal hybrid structures, Mater. Des. 92 (2016) 632–642.
[14] A.B. Abibe, S.T. Amancio-Filho, J.F. dos Santos, E. Hage, Mechanical and failure behaviour of hybrid polymer–metal staked joints, Mater. Des. 46 (2013) 338–347.
[15] H.-S. Park, T.-T. Nguyen, Numerical Simulation of Infrared Staking Plastic for an Automotive Part. ICCM2015, 2015 1–7.
[16] H.S. Park, T.T. Nguyen, Development of infrared staking process for an automotive part. IOP conference series:, Mater. Sci. Eng. 95 (2015) 012019.
[17] L. Blaga, R. Bancilă, J.F. dos Santos, S.T. Amancio-Filho, Friction riveting of glass–fibre-reinforced polyetherimide composite and titanium grade 2 hybrid joints, Mater. Des. 50 (2013) 825–829.
[18] J. Altmeyer, J.F. dos Santos, S.T. Amancio-Filho, Effect of the friction riveting process parameters on the joint formation and performance of Ti alloy/short-fibre reinforced polyether ether ketone joints, Mater. Des. 60 (2014) 164–176.
[19] H. Seidlitz, L. Ulke-Winter, L. Kroll, New joining technology for optimized metal/composite assemblies, J. Eng. 2014 (2014) 1–11.
[20] G. Marannano, B. Zuccarello, Numerical experimental analysis of hybrid double lap aluminum-CFRP joints, Compos. Part B 71 (2015) 28–39.
[21] B.M. İçten, R. Karakuzu, M.E. Toygar, Failure analysis of woven kevlar fiber reinforced epoxy composites pinned joints, Commun. Strateg. 73 (2006) 443–450.
[22] G. Di Franco, L. Fratini, A. Pasta, Influence of the distance between rivets in self-piercing riveting bonded joints made of carbon fiber panels and AA2024 blanks, Mater. Des. 35 (2012) 342–349.
[23] Z. Wang, S. Zhou, J. Zhang, X. Wu, L. Zhou, Progressive failure analysis of bolted single-lap composite joint based on extended finite element method, Mater. Des. 37 (2012) 582–588.
[24] F. Sen, M. Pakdil, O. Sayman, S. Benli, Experimental failure analysis of mechanically fastened joints with clearance in composite laminates under preload, Mater. Des. 29 (2008) 1159–1169.
[25] Y. Tao, G. Jiao, B. Wang, Y. Chang, Effect of Z-pins' diameter, spacing and overlap length on connecting performance of CMC single lap joint, Acta Mech. Solida Sin. 21 (2008) 461–471.
[26] R. Li, N. Huong, A. Crosky, A.P. Mouritz, D. Kelly, P. Chang, Improving bearing performance of composite bolted joints using z-pins, Compos. Sci. Technol. 69 (2009) 883–889.
[27] E. Ghafoori, M. Motavalli, Normal, high and ultra-high modulus carbon fiber-reinforced polymer laminates for bonded and un-bonded strengthening of steel beams, Mater. Des. 67 (2015) 232–243.
[28] Y. Zhou, K. Jiang, M. Gou, N. Li, P. Zhu, D. Wang, et al., Prediction of debonding strength of tensile hybrid bonded joints using fracture mechanics, Mater. Des. 61 (2014) 87–100.
[29] A.S. Bouchikhi, A. Megueni, S. Gouasmi, F.B. Boukoulda, Effect of mixed adhesive joints and tapered plate on stresses in retrofitted beams bonded with a fiber-reinforced polymer plate, Mater. Des. 50 (2013) 893–904.
[30] K.N. Anyfantis, N.G. Tsouvalis, Loading and fracture response of CFRP-to-steel adhesively bonded joints with thick adherents — part I: experiments, Commun. Strateg. 96 (2013) 850–857.
[31] H.K.D. Medlin, ASM Handbook Volume 8: Mechanical Testing and Evaluation: ASM International, 2000.
[32] H.S. da Costa Mattos, A.H. Monteiro, R. Palazzetti, Failure analysis of adhesively bonded joints in composite materials, Mater. Des. 33 (2012) 242–247.
[33] M. Kashfuddoja, M. Ramji, Assessment of local strain field in adhesive layer of an unsymmetrically repaired CFRP panel using digital image correlation, Int. J. Adhes. Adhes. 57 (2015) 57–69.
[34] K. Zhang, Z. Yang, Y. Li, A method for predicting the curing residual stress for CFRP/Al adhesive single-lap joints, Int. J. Adhes. Adhes. 46 (2013) 7–13.
[35] S. Akpinar, Effects of laminate carbon/epoxy composite patches on the strength of double-strap adhesive joints: experimental and numerical analysis, Mater. Des. 51 (2013) 501–512.
[36] M.-S. Seong, T.-H. Kim, K.-H. Nguyen, J.-H. Kweon, J.-H. Choi, A parametric study on the failure of bonded single-lap joints of carbon composite and aluminum, Commun. Strateg. 86 (2008) 135–145.
[37] J.-H. Kweon, J.-W. Jung, T.-H. Kim, J.-H. Choi, D.-H. Kim, Failure of carbon composite-to-aluminum joints with combined mechanical fastening and adhesive bonding, Commun. Strateg. 75 (2006) 192–198.
[38] R. Matsuzaki, M. Shibata, A. Todoroki, Improving performance of GFRP/aluminum single lap joints using bolted/co-cured hybrid method, Compos. A: Appl. Sci. Manuf. 39 (2008) 154–163.
[39] G. Kelly, Load transfer in hybrid (bonded/bolted) composite single-lap joints, Commun. Strateg. 69 (2005) 35–43.
[40] S. Gómez, J. Oñoro, J. Pecharromán, A simple mechanical model of a structural hybrid adhesive/riveted single lap joint, Int. J. Adhes. Adhes. 27 (2007) 263–267.
[41] N. Kashaev, V. Ventzke, S. Riekehr, F. Dorn, M. Horstmann, Assessment of alternative joining techniques for Ti–6Al–4V/CFRP hybrid joints regarding tensile and fatigue strength, Mater. Des. 81 (2015) 73–81.
[42] X. Wang, J. Ahn, J. Lee, B.R.K. Blackman, Investigation on failure modes and mechanical properties of CFRP-Ti6Al4V hybrid joints with different interface patterns using digital image correlation, Mater. Des. 101 (2016) 188–196.
[43] C.G. Pickin, K. Young, I. Tuersley, Joining of lightweight sandwich sheets to aluminium using self-pierce riveting, Mater. Des. 28 (2007) 2361–2365.
[44] F. Lambiase, Joinability of different thermoplastic polymers with aluminium AA6082 sheets by mechanical clinching, Int. J. Adv. Manuf. Technol. 80 (2015) 1995–2006.
[45] F. Lambiase, Mechanical behaviour of polymer-metal hybrid joints produced by clinching using different tools, Mater. Des. 87 (2015) 606–618.
[46] S. Lüder, S. Härtel, C. Binotsch, B. Awiszus, Influence of the moisture content on flat-clinch connection of wood materials and aluminium, J. Mater. Process. Technol. 214 (2014) 2069–2074.
[47] B.A. Behrens, R. Rolfes, M. Vucetic, J. Reinoso, M. Vogler, N. Grbic, Material modelling of short fiber reinforced thermoplastic for the FEA of a clinching test, Procedia CIRP. 18 (2014) 250–255.
[48] B.-A. Behrens, R. Rolfes, M. Vucetic, I. Peshekhodov, J. Reinoso, M. Vogler, et al., Material characterization for FEA of the clinching process of short fiber reinforced thermoplastics with an aluminum sheet, 6th International Conference on Tribology in Manufacturing Processes & Joining by Plastic Deformation 2014, pp. 557–568.
[49] C.-J. Lee, J.-M. Lee, H.-Y. Ryu, K.-H. Lee, B.-M. Kim, D.-C. Ko, Design of hole-clinching process for joining of dissimilar materials – Al6061-T4 alloy with DP780 steel, hot-pressed 22MnB5 steel, and carbon fiber reinforced plastic, J. Mater. Process. Technol. 214 (2014) 2169–2178.
[50] ASTM D5961, Standard Test Method for Bearing Response of Polymer Matrix Composite Laminates, ASTM International, West Conshohocken, PA, 2004.
[51] ASTM D3846, Standard Test Method for In-Plane Shear Strength of Reinforced Plastics, ASTM International, West Conshohocken, PA, 2015.
[52] F. Lambiase, Clinch joining of heat-treatable aluminum AA6082-T6 alloy under warm conditions, J. Mater. Process. Technol. 225 (2015) 421–432.
[53] F. Lambiase, A. Di Ilio, Damage analysis in mechanical clinching: experimental and numerical study, J. Mater. Process. Technol. 230 (2016) 109–120.
[54] J. Mucha, The analysis of lock forming mechanism in the clinching joint, Mater. Des. 32 (2011) 4943–4954.
[55] F. Lambiase, A. Di Ilio, A. Paoletti, Joining aluminium alloys with reduced ductility by mechanical clinching, Int. J. Adv. Manuf. Technol. 77 (2015) 1295–1304.

[56] F. Lambiase, Influence of process parameters in mechanical clinching with extensible dies, Int. J. Adv. Manuf. Technol. 66 (2013) 2123–2131.
[57] E.S. Research, T.C. Structures, M. Division, Structural Materials Handbook: Polymer Composites: European Space Agency, 1994.
[58] H. Ahmad, A.D. Crocombe, P.A. Smith, Strength prediction in CFRP woven laminate bolted single-lap joints under quasi-static loading using XFEM, Compos. A: Appl. Sci. Manuf. 66 (2014) 82–93.
[59] P.P. Camanho, L. Tong, Composite Joints and Connections: Principles, Modelling and Testing: Woodhead Publishing Limited, 2011.
[60] T. Keller, T. Vallée, Adhesively bonded lap joints from pultruded GFRP profiles. Part I: stress–strain analysis and failure modes, Compos. Part B 36 (2005) 331–340.
[61] G. Di Franco, L. Fratini, A. Pasta, Analysis of the mechanical performance of hybrid (SPR/bonded) single-lap joints between CFRP panels and aluminum blanks, Int. J. Adhes. Adhes. 41 (2013) 24–32.